

# Supramolecular Templating in Kirromycin Biosynthesis: The Acyltransferase KirCII Loads Ethylmalonyl-CoA Extender onto a Specific ACP of the *trans*-AT PKS

Ewa M. Musiol,<sup>1</sup> Thomas Härtner,<sup>1</sup> Andreas Kulik,<sup>1</sup> Jana Moldenhauer,<sup>2</sup> Jörn Piel,<sup>2</sup> Wolfgang Wohlleben,<sup>1</sup> and Tilmann Weber<sup>1,\*</sup>

<sup>1</sup>Eberhard-Karls-Universität Tübingen, Interfakultäres Institut für Mikrobiologie und Infektionsmedizin, Mikrobiologie/Biotechnologie, 72076 Tübingen, Germany

<sup>2</sup>Rheinische Friedrich-Wilhelms-Universität Bonn, Kekulé-Institut für Organische Chemie und Biochemie, 53121 Bonn, Germany

\*Correspondence: [tilmann.weber@biotech.uni-tuebingen.de](mailto:tilmann.weber@biotech.uni-tuebingen.de)

DOI 10.1016/j.chembiol.2011.02.007

## SUMMARY

In the biosynthesis of complex polyketides, acyltransferase domains (ATs) are key determinants of structural diversity. Their specificity and position in polyketide synthases (PKSs) usually controls the location and structure of building blocks in polyketides. Many bioactive polyketides, however, are generated by *trans*-AT PKSs lacking internal AT domains. They were previously believed to use mainly malonyl-specific free-standing ATs. Here, we report a mechanism of structural diversification, in which the *trans*-AT KirCII regiospecifically incorporates the unusual extender unit ethylmalonyl-CoA in kirromycin polyketide biosynthesis.

## INTRODUCTION

Many important bacterial drugs are synthesized by polyketide synthases (PKS), which work as assembly lines (Hertweck, 2009). Type I PKSs are large multifunctional enzymes, which have a complex, modular organization. Each PKS module contains a set of catalytic domains that perform one elongation step of the polyketide chain. A classical type I PKS module includes three essential domains—an acyltransferase (AT), a ketosynthase (KS), and an acyl carrier protein (ACP). The enzymatic role of ATs is the selection and loading of extender units, usually coenzyme A-activated carboxylic acids, onto *holo*-ACPs. The KS domain is responsible for the condensation of these building blocks in polyketide assembly. Further modifications during the chain elongation process are performed by optional domains, which are often present in such multifunctional enzymes and contribute to the high structural variability of their products. This variability is further increased by the ability to incorporate various extender units at the different modules. The extender unit specificity is conferred by the internal AT domains.

During the last decade, variants in the PKS architecture have been described, in which AT domains are not present in the megaenzyme but instead act as discrete enzymes (*trans*-AT

PKS type) (Staunton and Weissman, 2001; Piel, 2010). In most of such assembly lines, malonyl-CoA is used as extender unit, although the transfer of malonyl-CoA to ACPs by *trans*-acting ATs was biochemically confirmed only for leinamycin (Cheng et al., 2003), bacillaene (Calderone et al., 2006), and bryostatin (Lopanić et al., 2008). Whereas in *cis*-AT PKS different extender units are commonly incorporated, in *trans*-AT PKSs structural variability is enhanced by the frequent inclusion of additional modifying domains (e.g., methyltransferases into the PKS modules). Currently, there are only few reports of extender units different from malonyl-CoA in *trans*-AT pathways. For example, in oxazolomycin biosynthesis, the transfer of methoxymalonyl-CoA by OzmC was postulated on the basis of mutational analyses (Zhao et al., 2010). In the sorangicin biosynthetic pathway, the involvement of a discrete AT in loading hydroxymalonyl-CoA was proposed (Irschik et al., 2010).

Recently, the transfer of a (2*S*)-aminomalonyl extender unit to ACP1 of the PKS ZmaA has been described for zwittermixin biosynthesis (Chan and Thomas, 2010). In this case, the substrate for the AT ZmaA is already attached to the type II ACP ZmaH. To our knowledge, the direct loading of free, nonmalonate precursors by *trans*-ATs has not yet been biochemically confirmed.

In kirromycin biosynthesis, the incorporation of ethylmalonyl-CoA was suggested (Weber et al., 2008). This compound (Wolf et al., 1974) is the prototype member of the elfamycin family of antibiotics, which inhibit protein biosynthesis by interfering with the bacterial elongation factor EF-Tu. Interestingly, the producer strain *Streptomyces collinus* Tü 365 has a kirromycin sensitive EF-Tu (Olsthooorn-Tielemans et al., 2007). Nevertheless *S. collinus* is able to survive when the antibiotic is produced. Thus, there has to be a specific resistance mechanism that was not identified yet. Kirromycin is a narrow-spectrum antibiotic; it exhibits activity against, for example, streptococci, some enterococci, *Neisseria gonorrhoeae*, *Haemophilus influenzae*, and the malaria parasite *Plasmodium falciparum*.

The antibiotic is synthesized by a complex of type I PKS and nonribosomal peptide synthetases (Weber et al., 2008; Laiple et al., 2009). This assembly line is encoded by the genes *kirAI-kirAVI* and *kirB*. *KirAI-AV* are multifunctional enzymes of the *trans*-AT PKS type, whereas *KirAVI* belongs to the canonical

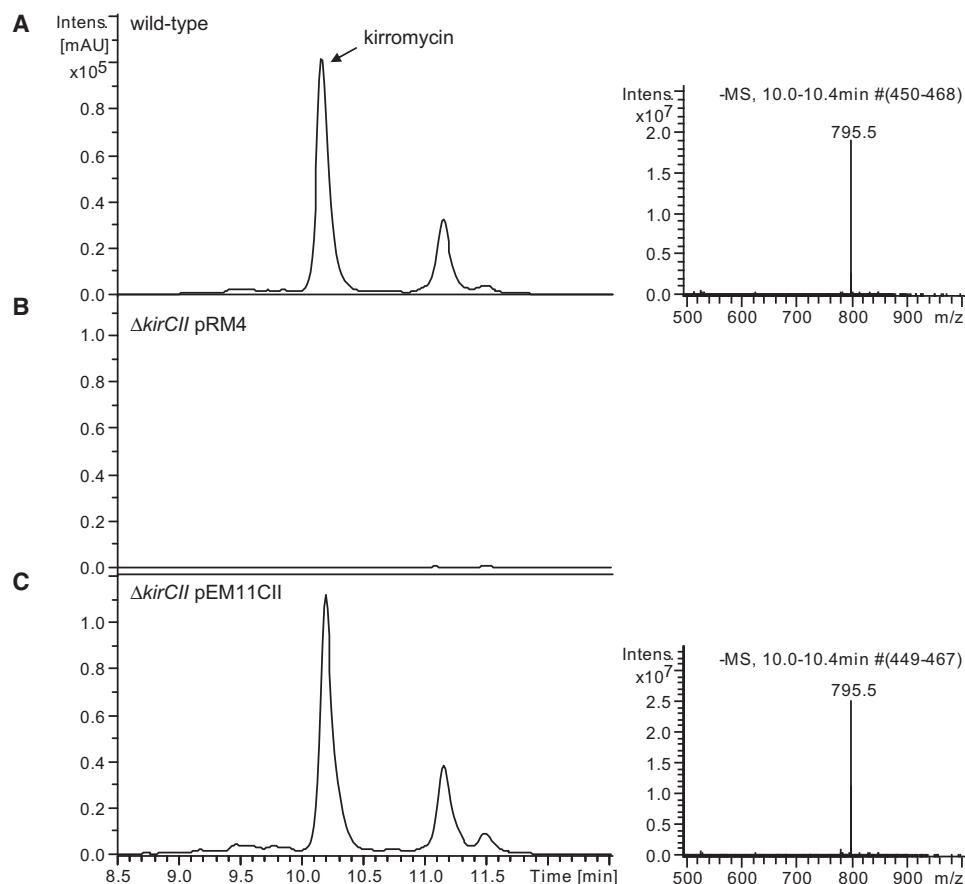


**Figure 1. Kirromycin Production Assay**

(A) HPLC/ESI-MS analysis of extracts of the wild-type *S. collinus* Tü 365. Left: HPLC UV/Vis trace. Right: mass spectrum of kirromycin (negative mode).

(B) HPLC/ESI-MS analysis of extracts of the mutant  $\Delta kirCII$  carrying the vector pRM4.

(C) HPLC/ESI-MS analysis of extracts of the complemented mutant  $\Delta kirCII$  pEM11CII. Left: HPLC UV/Vis trace. Right: mass spectrum of kirromycin (negative mode).

See also Figures S1 and S2.

*cis*-AT PKS type and contains internal AT domains (see Figure S1 available online). Such *cis* and *trans* AT-PKS mixtures are found very rarely (e.g., in the biosynthetic pathway of psymberin) (Fisch et al., 2009).

Although most condensation steps during the biosynthesis of the kirromycin carbon skeleton are performed with malonyl-CoA, at module 5 of KirAll, an ethylmalonyl-CoA unit is integrated. Thus, the question arises how the loading specificity of different extender units to the PKS is accomplished in kirromycin biosynthesis.

In the kirromycin gene cluster, two genes, *kirCI* and *kirCII*, encode putative ATs (Figure S1) (Weber et al., 2008). The *trans*-AT KirCI is similar to MmpC from *Pseudomonas fluorescens*, which seems to be the malonyl-CoA-specific AT in mupirocin biosynthesis (El Sayed et al., 2003; Thomas et al., 2010). KirCII is related to an AT domain in the stigmatellin *cis*-AT type PKS StiA (Gaitatzis et al., 2002) from *Stigmatella aurantiaca* (47% identity, 60% similarity, UniProt-Acc: Q8RJY6). In phylogenetic analyses, StiA is a member of a clade of mostly methylmalonyl-CoA-specific ATs that also contains *cis*-AT domains with other extender unit specificities. Because of this similarity, we

hypothesized that KirCII could have the required ethylmalonyl-CoA specificity.

## RESULTS AND DISCUSSION

To confirm the involvement of KirCII in the biosynthesis of kirromycin, a gene inactivation mutant was generated, in which the putative AT gene, *kirCII*, was replaced by a thiostrepton resistance cassette (see Supplemental Experimental Procedures). The genotype of the resultant mutant,  $\Delta kirCII$ , was confirmed by Southern hybridization and PCR (Figure S2). HPLC-MS analyses of culture extracts showed that this mutant lost its ability to produce kirromycin (Figures 1A and 1B). These results confirm that KirCII is essential for kirromycin biosynthesis. The complementation of the *kirCII* gene replacement mutant restored kirromycin production to the wild-type level (Figure 1C), showing that the lack of antibiotic production in the mutant was caused by the deletion of the *kirCII* gene and not by polar effects due to the incorporation of the resistance cassette. In contrast to leinamycin (Cheng et al., 2003) and virginiamycin (Pulsawat et al., 2007), where an overproduction

**Table 1. Effects of Overexpression of *kirCII* in the Wild-Type Kirromycin Producer Strain *Streptomyces collinus* Tü 365**

Strain	Kirromycin Concentration (mg/l), Mean $\pm$ SD
Wild-type <i>S. collinus</i> Tü 365	9.0 $\pm$ 1.0
<i>S. collinus</i> pRM4	14.0 $\pm$ 5.6
<i>S. collinus</i> pEM11CII	16.6 $\pm$ 9.4

of the discrete ATs led to increased antibiotics yields, the overexpression of *kirCII* in the wild-type *S. collinus* did not result in a significantly higher kirromycin production (Table 1). However, the high fluctuation of kirromycin yield in the *kirCII* overproduction strain might indicate detrimental effects of the overexpression on cell growth and thus may influence our observations.

For biochemical characterization of the substrate specificity of KirCII and its ability to transfer acyl-CoAs to selected ACPs, an in vitro ACP-loading assay was performed. This assay consists of two steps: first, *apo*-ACP to *holo*-ACP activation, and then, the loading of *holo*-ACPs by the *trans* AT KirCII. We selected ACP4 of module 4, which according to the structure of kirromycin should be a malonyl carrier, and ACP5 of module 5, for which ethylmalonyl incorporation was predicted (Weber et al., 2008). The *apo*-ACPs and the putative AT KirCII were expressed as His<sub>6</sub>-tagged fusion proteins and purified from *Escherichia coli* (Figure S3). The inactive *apo*-ACP4 and *apo*-ACP5 were converted to their functional *holo* forms by the phosphopantetheinyl transferase Sfp from *Bacillus subtilis* (Quadri et al., 1998) in the presence of CoA. Phosphopantetheinylation was monitored by HPLC and ESI-MS analysis until the *apo*-ACPs were fully activated. The resultant *holo*-ACPs were then used to determine the ACP-loading ability of KirCII for different CoA substrates malonyl-CoA, methylmalonyl-CoA, and ethylmalonyl-CoA. Because ethylmalonyl-CoA was not commercially available, unlabeled ethylmalonyl-CoA was synthesized according to Taoka et al. (1994).

Each *holo*-ACP and KirCII was incubated in the presence of the acyl-CoAs. The reactions were quenched by quick-freezing and were analyzed by HPLC/ESI-MS.

The loading assay of *holo*-ACP5 using KirCII and ethylmalonyl-CoA as substrate resulted in an additional UV peak in the HPLC-chromatogram (Figure 2B and Table 2). The mass of the new ACP species corresponded exactly to the calculated mass of ethylmalonyl-*holo*-ACP5 (mass for EM-*holo*-ACP5, 16702.7). This mass was never observed in control reactions without KirCII. These results confirm that the transfer activity was performed by the *trans*-AT KirCII. When using the MagTran protein deconvolution software (Zhang and Marshall, 1998) on the mass spectrometry data of the loading assay containing KirCII, EM-CoA and *holo*-ACP4, no mass peak of EM-ACP4 could be extrapolated. Only the mass of *holo*-ACP4 was present (Figure 2A). On manual inspection of the raw mass spec data, small peaks corresponding to ethylmalonylated ACP4 could be identified indicating a very weak loading also of ACP4 (Figure S6C; Table 2). These data show that KirCII strongly prefers *holo*-ACP5 over *holo*-ACP4 as the target carrier protein under the in vitro assay conditions and thus can distinguish between the ACPs of different PKS modules.

To confirm the predicted molecular weight of the ACPs and to ensure that the detected transfer activity in the ACP-loading assay was performed by KirCII and not by any copurified, contaminating transferases from *E. coli*, control reactions were performed. As a negative control, crude extracts of an *E. coli* strain carrying the empty pET expression plasmid were prepared and purified by the identical protocol as applied for KirCII. The enriched *E. coli* proteins, termed “pET52-proteins,” and KirCII, respectively, were added to the *holo*-ACPs. In the negative control, in which the “pET52-proteins” were tested, no transfer activity was present. As positive control, acyl-phosphopantetheinyl-groups were directly transferred to *apo*-ACPs by Sfp, which has low specificity toward its CoA-substrates (Sunbul et al., 2009). The products obtained in the positive control reactions corresponded to the calculated masses of loaded *holo*-ACPs and were used as a reference for successful transfer (Figures S4 and S5; Table 2). Additionally, to exclude self-loading of *holo*-ACPs, which was described for type II PKS and the fatty acid ACPs PfACP and BnACP (Arthur et al., 2006; Misra et al., 2007), both ACPs, *holo*-ACP4 and *holo*-ACP5, without KirCII, were incubated with the tested substrates. No loading activity was observed in these samples.

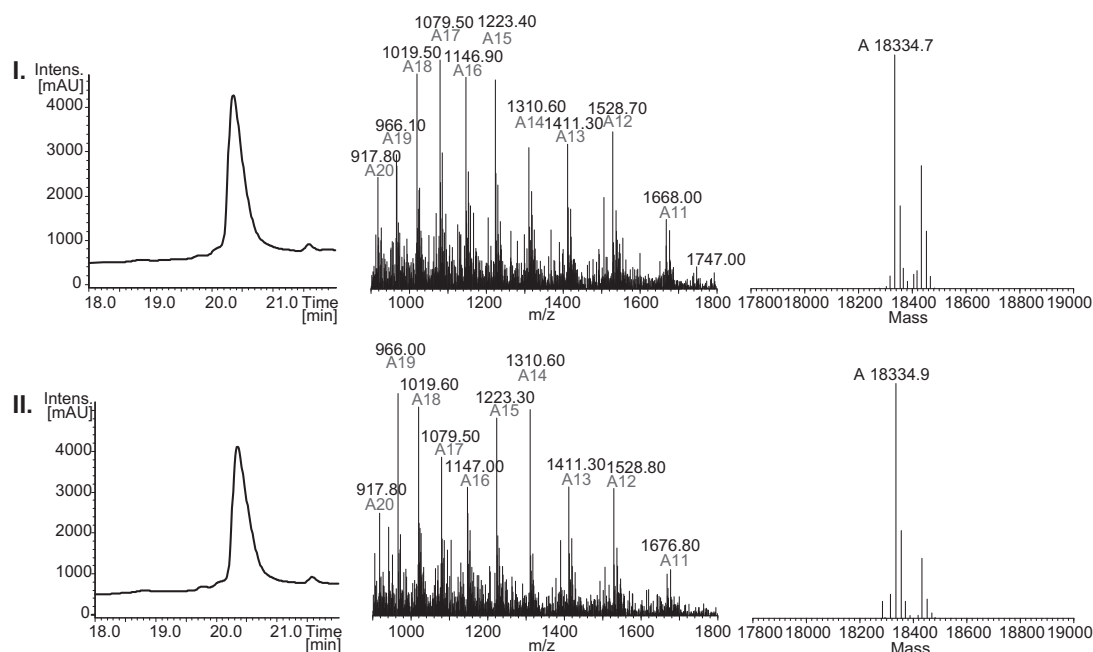
To further narrow down the specificity of KirCII, also the typical PKS extender units malonyl- and methylmalonyl-CoA were tested. For both substrates, no transfer activity of KirCII to either ACP4 and ACP5 was detected by HPLC-MS. Only *holo*-ACP masses were found in those reactions (Figures S6A, S6B, and S7; Table 2).

In addition to the HPLC-MS-based assay, autoradiography was used as a second, more sensitive detection method. To perform this assay, the samples including ACPs were incubated with <sup>14</sup>C-labeled malonyl-CoA or methylmalonyl-CoA. The reactions were quenched by addition of cold acetone and subjected to SDS-PAGE and phosphorimaging (Figure 3). The loading assay was performed with the same ACPs and control reactions described above. The autoradiogram displayed clear signals for the positive controls, showing that Sfp loaded the <sup>14</sup>C-substrate directly onto the *apo*-ACPs. No loading activity was detected in the negative controls, where the *holo*-ACPs were incubated with “pET52-proteins” in the absence of KirCII. Also in the presence of KirCII, no transfer of [1,3-<sup>14</sup>C]-malonyl and [1,3-<sup>14</sup>C]-methylmalonyl, respectively, was observed.

## SIGNIFICANCE

**Our results, confirmed by two different methods, demonstrate that the *trans*-AT KirCII is not able to use malonyl- or methylmalonyl-CoA to load the tested acyl carrier proteins. Therefore, the ethylmalonyl-loading KirCII represents the first biochemically characterized discrete AT with proven specificity and ACP-loading activity for a non-malonyl unit. Kirromycin is synthesized as a main component of *Streptomyces collinus* Tü 365, and no derivatives are reported in which ethylmalonyl-CoA is incorporated at other positions of the molecule backbone. Thus, the recognition mechanism that results in the specific interaction of the AT KirCII with the ACP of module 5 is at least in part governed by the ACP. Protein template-directed docking of free-standing proteins that provide building blocks is an**

## A ACP4



## B ACP5

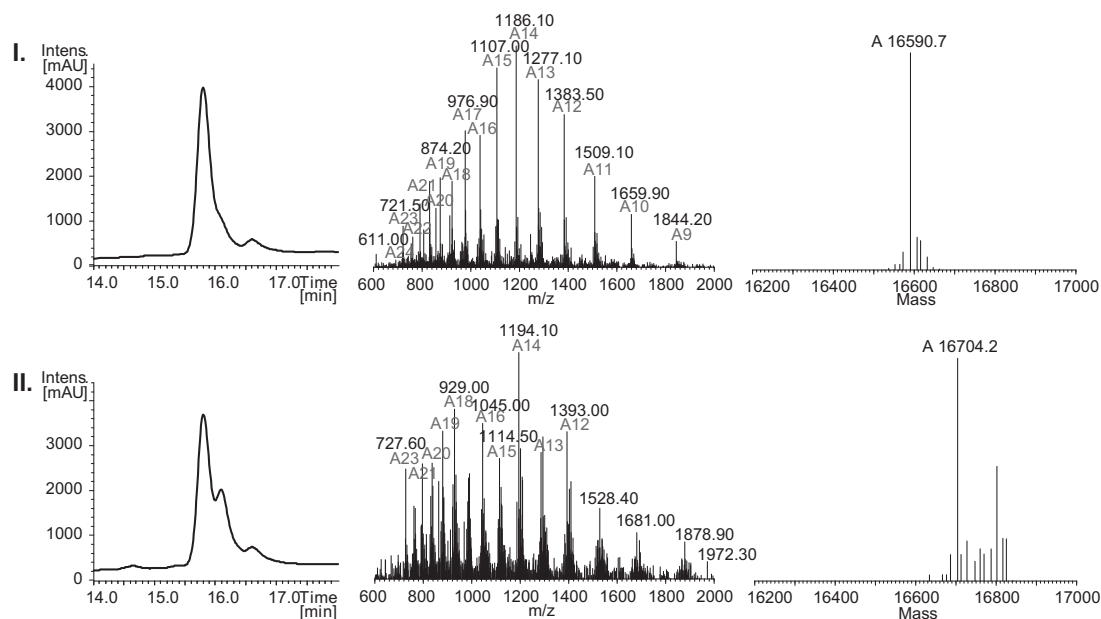


**Figure 2. HPLC/ESI-MS Analysis of the ACP4/ACP5-Loading Assay with Ethylmalonyl-CoA as Substrate for KirCII**

(A) ACP4.

(B) ACP5.

(I) Negative control containing ACP4/ACP5, pET52-proteins, no KirCII. (II) Loading assay containing ACP4/ACP5, ethylmalonyl-CoA, and KirCII. Left: HPLC UV/Vis trace. Central: mass spectrum. Right: deconvoluted spectrum generated with MagTran 1.03 (Zhang and Marshall, 1998).

See also Figures S3, S6, and S7.

**Table 2. Mass Spectrometric Analysis of In Vitro ACP Loading**

Sample <sup>a</sup>	Detected Mass <sup>b</sup>	Standard Deviation <sup>b</sup>	Calculated Mass
<b>ACP4</b>			
<i>apo</i> -ACP4	17993.7	0.8	17992.1
<i>holo</i> -ACP4 (Sfp loading, pos. control)	18333.9	0.8	18332.5
M- <i>holo</i> -ACP4 (Sfp loading, pos. control)	18420.7	1.8	18418.5
MM- <i>holo</i> -ACP4 (Sfp loading, pos. control)	18434.6	1.6	18432.5
EM- <i>holo</i> -ACP4 (Sfp loading, pos. control)	18449.1	1.9	18446.6
M- <i>holo</i> -ACP4 (KirCII loading)	Not detected	—	18418.5
MM- <i>holo</i> -ACP4 (KirCII loading)	Not detected	—	18446.6
EM- <i>holo</i> -ACP4 (KirCII loading)	(18446.2) <sup>c</sup>	8.4	18446.6
<b>ACP5</b>			
<i>apo</i> -ACP5	16249.6	0.5	16248.3
<i>holo</i> -ACP5 (Sfp loading, pos. control)	16589.8	1.2	16588.6
M- <i>holo</i> -ACP5 (Sfp loading, pos. control)	16674.6	1.3	16674.6
MM- <i>holo</i> -ACP5 (Sfp loading, pos. control)	16688.3	1.4	16688.7
EM- <i>holo</i> -ACP5 (Sfp loading, pos. control)	16704.7	1.2	16702.7
M- <i>holo</i> -ACP5 (KirCII loading)	Not detected	—	16674.6
MM- <i>holo</i> -ACP5 (KirCII loading)	Not detected	—	16688.7
EM- <i>holo</i> -ACP5 (KirCII loading)	16703.9	1.2	16702.7

See also Figures S4 and S5.

<sup>a</sup> M-*holo*-ACP: malonyl-*holo*-ACP, MM-*holo*-ACP: methylmalonyl-*holo*-ACP, EM-*holo*-ACP: ethylmalonyl-*holo*-ACP.

<sup>b</sup> Charge deconvolution/mass determination was performed with the ESIprot (Winkler, 2010) software.

<sup>c</sup> Small peaks of EM-*holo*-ACP4, which were not present in the control reaction, could only be detected manually in the protein ms data.

alternative mechanism to achieve structural diversity in polyketides. KirCII is a novel example of such supramolecular templating in antibiotic biosynthesis. This enzyme and its ethylmalonyl-CoA specificity can now provide conceptually novel opportunities to genetically engineer the structural diversity of polyketides.

## EXPERIMENTAL PROCEDURES

For general methods, strains, and cultivations see Supplemental Experimental Procedures.

### Generation of the *kirCII* Gene Inactivation Mutant $\Delta$ *kirCII*

Flanking regions of *kirCII* with sizes of 2 kb were amplified using cosmid 1C24 (Weber et al., 2008) as template and the primers l*kirCII*-5Eco, l*kirCII*-3Xba, r*kirCII*-5Xba, and r*kirCII*-3Hind (for primer sequences and PCR programs, see section II.10 of Supplemental Experimental Procedures). A thiostrepton resistance cassette from plasmid pSLE60 and the promoter region of the erythromycin resistance gene, *P<sub>ermE</sub>* from the vector pRM4 (Menges et al., 2007) were amplified with corresponding primers, thio5'Xba, thio3'Bgl2fuse and fuseBglermE5', ermE3'Xba, respectively. To achieve a fusion of the resulting products, *thioR* and *P<sub>ermE</sub>*, a second PCR using these fragments and the primers thio5'Xba and ermE3'Xba was performed. The fused amplicon *thioRP<sub>ermE</sub>* and the PCR products, l*kirCII* and r*kirCII* were individually cloned into pDrive (QIAGEN). l*kirCII* was excised from pDrive with EcoRI and XbaI and cloned into the EcoRI/XbaI-digested pA18mob, yielding pA18-l*kirCII*. Subsequently, r*kirCII* was introduced into this plasmid by XbaI/HindIII restriction and ligation, yielding pA18-lr*kirCII*. To clone the *thioRP<sub>ermE</sub>* cassette between the two fragments of pA18-lr*kirCII*, the *thioRP<sub>ermE</sub>* was inserted into the XbaI side of pA18-lr*kirCII*. The correct orientation of the *thioRP<sub>ermE</sub>* cassette was confirmed by control restrictions of the obtained plasmid pEM10*ΔCII*. A double crossover mutant was generated according to methods described by Weber et al. (2008) and verified by PCR with primers CIIintern1 and CIIintern2 and Southern hybridization.

### Complementation of the Mutant $\Delta$ *kirCII* and Homologous Expression of *kirCII* in *S. collinus* Tü 365

The *kirCII* gene of *S. collinus* Tü 365 was amplified from cosmid 1C24 using the primers YTKirCII-NdeStrep-5' and YTKirCII-Hind-3' (for primer sequences, see section II.10 of Supplemental Experimental Procedures) and was cloned into the vector pRM4, resulting in the plasmid pEM11CII (for detailed cloning procedures, see Supplemental Experimental Procedures). Intergeneric conjugation was used to transfer the plasmids pRM4 (negative control) and pEM11CII into the gene inactivation mutant  $\Delta$ *kirCII* and the wild-type strain *S. collinus* Tü 365.

### Protein Expression and Purification

ACP4, ACP5, and *kirCII* were amplified by PCR (for primers, see section II.10 of Supplemental Experimental Procedures) and were cloned into the vector pET-52 3C/LIC. The protein expression was performed in the *E. coli* strain Rosetta2(DE3)pLysS under different conditions (see section II.11 of Supplemental Experimental Procedures). The proteins ACP4, ACP5, and KirCII were purified by Ni-NTA affinity chromatography and ion exchange chromatography according to section II.6 of Supplemental Experimental Procedures.

### ACP-Loading Assay

To investigate the substrate specificity and ACP-loading ability of KirCII, an in vitro assay was established. The ACP-loading assay was performed in two steps, the *apo*- to *holo*-ACP phosphopantetheinylation and *holo*-ACP-loading by KirCII.

### In Vitro Activation of *apo*-ACP to *holo*-ACP

ACPs expressed in *E. coli* were purified as nonphosphopantetheinylated *apo*-ACPs. To apply them in the loading assay, a conversion to their active *holo*-ACP form is necessary. The *apo*-ACP activation was performed using the *B. subtilis* phosphopantetheinyl transferase Sfp in presence of coenzyme A. The phosphopantetheinylation reaction contained following components: 100  $\mu$ M *apo*-ACP4/5, 10–15  $\mu$ M Sfp, 0.8–1 mM coenzyme A (Sigma), and 50–60 mM MgCl<sub>2</sub> in final volume of 400  $\mu$ l (reaction buffer: 50 mM Tris-HCl



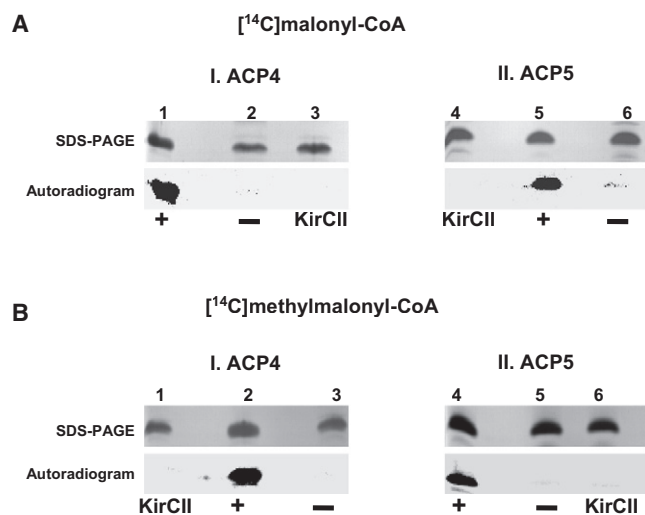


**Figure 3. Autoradiographic Analysis of the ACP4/ACP5-Loading Assay with  $[^{14}\text{C}]$ malonyl-/ $[^{14}\text{C}]$ methylmalonyl-CoA as Substrates for KirCII**

(A) Coomassie Brilliant Blue–stained gels and autoradiograms of the (I) ACP4- and (II) ACP5-loading assay with  $[^{14}\text{C}]$ malonyl-CoA. Lane 1: positive control reaction for ACP4 containing apo-ACP4 and Sfp (detected signal is  $[^{14}\text{C}]$ malonyl-holo-ACP4); lane 2: negative control for holo-ACP4 containing pET52-proteins, no KirCII; lane 3: holo-ACP4 and KirCII; lane 4: holo-ACP5 and KirCII; lane 5: positive control reaction for ACP5 containing apo-ACP5 and Sfp (detected signal is  $[^{14}\text{C}]$ malonyl-holo-ACP5); lane 6: negative control for holo-ACP5 containing pET52-proteins, no KirCII.

(B) Coomassie Brilliant Blue–stained gels and autoradiograms of the (I) ACP4- and (II) ACP5- loading assay with  $[^{14}\text{C}]$ methylmalonyl-CoA. Lane 1: holo-ACP4 and KirCII; lane 2: positive control reaction for ACP4 containing apo-ACP4 and Sfp (detected signal is  $[^{14}\text{C}]$ methylmalonyl-holo-ACP4); lane 3: negative control for holo-ACP4 containing pET52-proteins, no KirCII; lane 4: positive control reaction for ACP5 containing apo-ACP5 and Sfp (detected signal is  $[^{14}\text{C}]$ methylmalonyl-holo-ACP5); lane 5: negative control for holo-ACP5 containing pET52-proteins, no KirCII; lane 6: holo-ACP5 and KirCII. See also Figure S3.

[pH 7.5]). The mixture was incubated first for 1 hr at 37°C and then at 4°C until complete conversion to holo-ACPs was achieved. The reaction was monitored by HPLC/ESI-MS.

#### In Vitro ACP-Loading Catalyzed by KirCII

To study the ability of KirCII to acylate various acyl carrier proteins, the holo-ACPs were incubated with KirCII and acyl-CoA precursors. The reactions were analyzed by HPLC/ESI-MS or autoradiography analysis.

#### HPLC/ESI-MS Analysis

Malonyl-CoA was obtained from Fluka, and methylmalonyl-CoA was obtained from Sigma. Ethylmalonyl-CoA was synthesized according to Taoka et al. (1994).

A typical reaction was performed in reaction buffer (50 mM Tris-HCl [pH 7.5]) with 80  $\mu\text{M}$  holo-ACP (20  $\mu\text{l}$  of the phosphopantetheinylation reaction, see above), 3  $\mu\text{M}$  KirCII, 500  $\mu\text{M}$  substrate, and 50 mM  $\text{MgCl}_2$  in a volume of 25  $\mu\text{l}$ . In negative controls, KirCII was replaced by the same amount of pET52-proteins. As positive control, direct loading of acyl phosphopantetheinyl moieties to apo-ACPs by Sfp was used. This resulted in formation of holo-ACPs and acylated holo-ACPs (malonyl-holo-ACPs, methylmalonyl-holo-ACPs, and ethylmalonyl-holo-ACPs). The ACP-loading assay samples were incubated at 37°C for 30 min, the reactions were quenched by freezing at  $-80^\circ\text{C}$ , and samples were stored at  $-80^\circ\text{C}$  until HPLC/ESI-MS analysis.

#### Autoradiography Analysis

The ACP-loading assay was performed with  $[^{14}\text{C}]$ malonyl-CoA and  $[^{14}\text{C}]$ methylmalonyl-CoA. The chemicals,  $[1,3\text{-}^{14}\text{C}]$ malonyl coenzyme A (50–60 mCi/mmol, 1.85–2.22 GBq/mmol) and  $[1,3\text{-}^{14}\text{C}]$ methylmalonyl coenzyme A, (50–60 mCi/mmol and 1.85–2.22 GBq/mmol) were purchased from BIOTREND Chemikalien. To apply various substrate concentrations, the radiolabeled acyl-CoA derivatives were used directly or diluted with the reaction buffer. In general, the reactions contained 10  $\mu\text{M}$  holo-ACP (2.5  $\mu\text{l}$  of the phosphopantetheinylation reaction), 50 mM  $\text{MgCl}_2$ , 7–20  $\mu\text{M}$   $[^{14}\text{C}]$ -labeled substrate, and 0.4–0.7  $\mu\text{M}$  KirCII in 25  $\mu\text{l}$  using 50 mM Tris-HCl (pH 7.5) as reaction buffer. As positive control reaction direct transfer of the acyl-CoAs to apo-ACPs by the unspecific phosphopantetheinyl transferase Sfp was monitored. The negative control was performed with pET52-proteins instead of KirCII. The reactions were incubated at 37°C for 30 min and quenched by the addition of cold acetone (900  $\mu\text{l}$ ). Proteins were precipitated by centrifugation (10 min, 27750 g, Sorvall RC6 PLUS), resolved in 2 $\times$  sampler buffer, separated on 12% SDS-PAGE, and blotted onto a nitrocellulose membrane (BioTrace, pure nitrocellulose, Pall). The membrane was dried on air for 24 hr and placed into a light tight exposure cassette (Amersham Biosciences) with a storage phosphor screen (GE Healthcare). After 2 days of incubation time, the exposed phosphor screen was scanned using Typhoon TRIO+ Variable Mode Imager, (GE Healthcare) and was analyzed by the software ImageQuant TL (GE Healthcare).

#### SUPPLEMENTAL INFORMATION

Supplemental information includes seven figures and Supplemental Experimental Procedures, and can be found with this article online at doi:10.1016/j.chembiol.2011.02.007.

#### ACKNOWLEDGMENTS

We would like to thank Dr. Z. Zhang for providing the MagTran 1.03 software. This work was funded by the BMBF grants GenoMikPlus/GenBioCom (FKZ0313805J/FKZ0315585A/FKZ0315581I) to W.W. and T.W. and J.P. and by the DFG (SFB 642 to J.P.). The authors declare no competing financial interests. E.-M.M. performed the majority of the wet lab experiments and data evaluation with guidance from W.W. and T.W. and wrote the manuscript. T.H. performed the production assays. A.K. carried out the HPLC-ESI-MS analyses. J.M. and J.P. synthesized ethylmalonyl-CoA. J.P., W.W., and T.W. contributed to the manuscript.

Received: January 17, 2011

Revised: February 14, 2011

Accepted: February 15, 2011

Published: April 21, 2011

#### REFERENCES

- Arthur, C.J., Szafranska, A.E., Long, J., Mills, J., Cox, R.J., Findlow, S.C., Simpson, T.J., Crump, M.P., and Crosby, J. (2006). The malonyl transferase activity of type II polyketide synthase acyl carrier proteins. *Chem. Biol.* 13, 587–596.
- Calderone, C.T., Kowtoniuk, W.E., Kelleher, N.L., Walsh, C.T., and Dorrestein, P.C. (2006). Convergence of isoprene and polyketide biosynthetic machinery: isoprenyl-S-carrier proteins in the *pksX* pathway of *Bacillus subtilis*. *Proc. Natl. Acad. Sci. USA* 103, 8977–8982.
- Chan, Y.A., and Thomas, M.G. (2010). Recognition of (2S)-aminomalonyl-acyl carrier protein (ACP) and (2R)-hydroxymalonyl-ACP by acyltransferases in zwittermixin A biosynthesis. *Biochemistry* 49, 3667–3677.
- Cheng, Y.Q., Tang, G.L., and Shen, B. (2003). Type I polyketide synthase requiring a discrete acyltransferase for polyketide biosynthesis. *Proc. Natl. Acad. Sci. USA* 100, 3149–3154.
- El Sayed, A.K., Hotherhall, J., Cooper, S.M., Stephens, E., Simpson, T.J., and Thomas, C.M. (2003). Characterization of the mupirocin biosynthesis gene cluster from *Pseudomonas fluorescens* NCIMB 10586. *Chem. Biol.* 10, 419–430.

- Fisch, K.M., Gurgui, C., Heycke, N., van der Sar, S.A., Anderson, S.A., Webb, V.L., Taudien, S., Platzer, M., Rubio, B.K., Robinson, S.J., et al. (2009). Polyketide assembly lines of uncultivated sponge symbionts from structure-based gene targeting. *Nat. Chem. Biol.* 5, 494–501.
- Gaitatzis, N., Silakowski, B., Kunze, B., Nordsiek, G., Blöcker, H., Höfle, G., and Müller, R. (2002). The biosynthesis of the aromatic myxobacterial electron transport inhibitor stigmatellin is directed by a novel type of modular polyketide synthase. *J. Biol. Chem.* 277, 13082–13090.
- Hertweck, C. (2009). The biosynthetic logic of polyketide diversity. *Angew. Chem. Int. Ed. Engl.* 48, 4688–4716.
- Irschik, H., Kopp, M., Weissman, K.J., Buntin, K., Piel, J., and Müller, R. (2010). Analysis of the sorangicin gene cluster reinforces the utility of a combined phylogenetic/retrobiosynthetic analysis for deciphering natural product assembly by trans-AT PKS. *ChemBiochem* 11, 1840–1849.
- Laiple, K.J., Härtner, T., Fiedler, H.-P., Wohlleben, W., and Weber, T. (2009). The kirromycin gene cluster of *Streptomyces collinus* Tü 365 codes for an aspartate- $\alpha$ -decarboxylase, KirD, which is involved in the biosynthesis of the precursor  $\beta$ -alanine. *J. Antibiot. (Tokyo)* 62, 465–468.
- Lopanik, N.B., Shields, J.A., Buchholz, T.J., Rath, C.M., Hothersall, J., Haygood, M.G., Hakansson, K., Thomas, C.M., and Sherman, D.H. (2008). In vivo and in vitro trans-acylation by BryP, the putative bryostatin pathway acyltransferase derived from an uncultured marine symbiont. *Chem. Biol.* 15, 1175–1186.
- Menges, R., Muth, G., Wohlleben, W., and Stegmann, E. (2007). The ABC transporter Tba of *Amycolatopsis balhimycin* is required for efficient export of the glycopeptide antibiotic balhimycin. *Appl. Microbiol. Biotechnol.* 77, 125–134.
- Misra, A., Sharma, S.K., Surolia, N., and Surolia, A. (2007). Self-acylation properties of type II fatty acid biosynthesis acyl carrier protein. *Chem. Biol.* 14, 775–783.
- Olsthoorn-Tieleman, L.N., Palstra, R.J., van Wezel, G.P., Bibb, M.J., and Pleij, C.W. (2007). Elongation factor Tu3 (EF-Tu3) from the kirromycin producer *Streptomyces ramocissimus* is resistant to three classes of EF-Tu-specific inhibitors. *J. Bacteriol.* 189, 3581–3590.
- Piel, J. (2010). Biosynthesis of polyketides by trans-AT polyketide synthases. *Nat. Prod. Rep.* 27, 996–1047.
- Pulsawat, N., Kitani, S., and Nihira, T. (2007). Characterization of biosynthetic gene cluster for the production of virginiamycin M, a streptogramin type A antibiotic, in *Streptomyces virginiae*. *Gene* 393, 31–42.
- Quadri, L.E., Weinreb, P.H., Lei, M., Nakano, M.M., Zuber, P., and Walsh, C.T. (1998). Characterization of Sfp, a *Bacillus subtilis* phosphopantetheinyl transferase for peptidyl carrier protein domains in peptide synthetases. *Biochemistry* 37, 1585–1595.
- Staunton, J., and Weissman, K.J. (2001). Polyketide biosynthesis: a millennium review. *Nat. Prod. Rep.* 18, 380–416.
- Sunbul, M., Zhang, K., and Yin, J. (2009). Chapter 10: Using phosphopantetheinyl transferases for enzyme posttranslational activation, site specific protein labeling and identification of natural product biosynthetic gene clusters from bacterial genomes. *Methods Enzymol.* 458, 255–275.
- Taoka, S., Padmakumar, R., Lai, M.T., Liu, H.W., and Banerjee, R. (1994). Inhibition of the human methylmalonyl-CoA mutase by various CoA-esters. *J. Biol. Chem.* 269, 31630–31634.
- Thomas, C.M., Hothersall, J., Willis, C.L., and Simpson, T.J. (2010). Resistance to and synthesis of the antibiotic mupirocin. *Nat. Rev. Microbiol.* 8, 281–289.
- Weber, T., Laiple, K.J., Pross, E.K., Textor, A., Grond, S., Welzel, K., Pelzer, S., Vente, A., and Wohlleben, W. (2008). Molecular analysis of the kirromycin biosynthetic gene cluster revealed  $\beta$ -alanine as precursor of the pyridone moiety. *Chem. Biol.* 15, 175–188.
- Winkler, R. (2010). ESIprot: a universal tool for charge state determination and molecular weight calculation of proteins from electrospray ionization mass spectrometry data. *Rapid Commun. Mass Spectrom.* 24, 285–294.
- Wolf, H., Chinali, G., and Parmeggiani, A. (1974). Kirromycin, an inhibitor of protein biosynthesis that acts on elongation factor Tu. *Proc. Natl. Acad. Sci. USA* 71, 4910–4914.
- Zhang, Z., and Marshall, A.G. (1998). A universal algorithm for fast and automated charge state deconvolution of electrospray mass-to-charge ratio spectra. *J. Am. Soc. Mass Spectrom.* 9, 225–233.
- Zhao, C., Coughlin, J.M., Ju, J., Zhu, D., Wendt-Pienkowski, E., Zhou, X., Wang, Z., Shen, B., and Deng, Z. (2010). Oxazolomycin biosynthesis in *Streptomyces albus* JA3453 featuring an “acyltransferase-less” type I polyketide synthase that incorporates two distinct extender units. *J. Biol. Chem.* 285, 20097–20108.